PROCEEDINGS OF SPIE

SPIEDigitalLibrary.org/conference-proceedings-of-spie

Optimization of InGaN quantum well interfaces for fast interwell carrier transport and low nonradiative recombination

Rinat Yapparov, Cheyenne Lynsky, Yi-Chao Chow, Shuji Nakamura, James Speck, et al.

Rinat Yapparov, Cheyenne Lynsky, Yi-Chao Chow, Shuji Nakamura, James S. Speck, Saulius Marcinkevičius, "Optimization of InGaN quantum well interfaces for fast interwell carrier transport and low nonradiative recombination," Proc. SPIE 12001, Gallium Nitride Materials and Devices XVII, 1200104 (5 March 2022); doi: 10.1117/12.2608695



Event: SPIE OPTO, 2022, San Francisco, California, United States

Optimization of InGaN quantum well interfaces for fast interwell carrier transport and low nonradiative recombination

Rinat Yapparov^a, Cheyenne Lynsky^b, Yi-Chao Chow^b, Shuji Nakamura^b, James S. Speck^b, and Saulius Marcinkevičius^a

^aDepartment of Applied Physics, KTH Royal Institute of Technology, 10691 Stockholm, Sweden; ^bMaterials Department, University of California, Santa Barbara, California 93106, USA

ABSTRACT

Efficient high-power operation of light emitting diodes based on InGaN quantum wells (QWs) requires rapid interwell hole transport and low nonradiative recombination. The transport rate can be increased by replacing GaN barriers with that of InGaN. Introduction of InGaN barriers, however, increases the rate of the nonradiative recombination. In this work, we have attempted to reduce the negative impact of the nonradiative recombination by introducing thin GaN or AlGaN interlayers at the QW/barrier interfaces. The interlayers, indeed, reduce the nonradiative recombination rate and increase the internal quantum efficiency by about 10%. Furthermore, the interlayers do not substantially slow down the interwell hole transport; for 0.5 nm Al_{0.10}Ga_{0.90}N interlayers the transport rate has even been found to increase. Another positive feature of the interlayers is narrowing of the QW PL linewidth, which is attributed to smoother QW interfaces and reduced fluctuations of the QW width.

Keywords: InGaN, quantum wells, LED, carrier transport, nonradiative recombination, internal quantum efficiency

1. INTRODUCTION

High-power operation of GaN-based light emitting diodes (LEDs) with In_xGa_{1-x}N quantum wells (QWs) requires high carrier densities in the active region. These high densities are achieved at high injection currents at which the internal quantum efficiency is primarily reduced by Auger recombination.¹ A straightforward way to reduce the carrier concentration in the QWs while maintaining the high LED output power would be to increase the number of QWs. Following this approach, LEDs with an active region containing large number of QWs (e.g., ten^{2,3}) have been used. However, subsequent studies have suggested that for InGaN QWs with GaN barriers operating in the visible spectral region the light emission originates from only one or two QWs closest to the *p*-side of the structure.^{4,5} This effect was attributed to the poor interwell (IW) hole transport.

In our previous study we have shown that in InGaN multiple QW structures at room temperature the IW transport is thermionic, and the limiting factor for the efficient transport and uniform IW carrier distribution is the thermionic emission of holes out of the QWs.⁶ Since the thermionic emission time depends exponentially on the barrier height, lowering this height by replacing GaN barriers with that of InGaN increases the IW transport rate.^{6,7} However, the InGaN barriers induce additional nonradiative Shockley-Read-Hall recombination centers, presumably at QW interfaces.⁷ In this work, we explore whether thin GaN or AlGaN layers grown at the QW interfaces could reduce this nonradiative recombination, and what would be the effect of such layers on the IW transport.

2. EXPERIMENTAL DETAILS

The study was performed on two groups of samples grown on *c*-plane sapphire substrate by metal-organic chemical vapor deposition. The first group contained identical QWs with or without the interlayers (Fig. 1(a)) and was used to study carrier recombination and internal quantum efficiency (IQE). These structures consisted of 4.3 µm GaN buffer layer, an active region with four 3 nm thick In_{0.12}Ga_{0.88}N QWs surrounded by different types of barriers, and a 100 nm GaN cap layer. The barriers were either purely In_{0.04}Ga_{0.96}N (reference sample) or contained 0.5 nm or 1.0 nm Al_{0.10}Ga_{0.90}N or GaN interlayers on both sides of the QW. The total barrier thickness (barrier plus interlayers) was always 8 nm. The second group of samples, used for the IW transport measurements, was identical to the first group but with an additional In_{0.18}Ga_{0.82}N detector QW (DQW) between the active region and the buffer layer (Fig. 1(a)). The DQW served as an optical marker for

Gallium Nitride Materials and Devices XVII, edited by Hiroshi Fujioka, Hadis Morkoç, Ulrich T. Schwarz, Proc. of SPIE Vol. 12001, 1200104 © 2022 SPIE ⋅ 0277-786X ⋅ doi: 10.1117/12.2608695

carriers that were excited in the cap layer and transferred through the four transport QWs (TQWs). ^{6,8,9} Emission of the TQWs was in the region of 410-420 nm; the photoluminescence (PL) peak of the DQWs was between 477-489 nm. The structures were unintentionally n-doped with an electron concentration of about 1×10^{17} cm⁻³. The threading dislocation density was $\sim 5 \times 10^8$ cm⁻².

Time-integrated and time-resolved PL measurements were performed in the 4-300 K temperature range. PL excitation was done by either 2nd or 3rd harmonic pulses of 200 fs duration from a self-mode-locking Ti:sapphire laser at 260 nm and 390 nm central wavelengths. Resonant excitation directly into the QWs at 390 nm was used for samples without the DQW and allowed to evaluate the radiative and nonradiative recombination times in the TQWs. The IW carrier transport was studied using 260 nm excitation wavelength, for which carriers were excited primarily in the GaN cap layer. Due to the concentration gradient, these carriers propagated further through the TQW region until they reached the DQW. Time resolved PL from the DQW, selected with appropriate band pass filters, was used to analyze dynamics of the IW carrier transport. Since the DQW PL decay time was much longer than the time interval of 12.5 ns between the pulses of the Ti:sapphire laser (80 MHz pulse repetition rate), an acousto-optic pulse picker was used to reduce the pulse repetition rate down to 4 MHz. Time-resolved PL transients were registered using a time-correlated single photon counter with the temporal response of 50 ps. Time-integrated PL spectra were recorded by a spectrometer with a liquid nitrogen-cooled charge-coupled device detector array.

3. RESULTS AND DISCUSSION

DQW PL transients of the transport samples at 300 K are presented in Figure 1(b). The transients contain a fast and slow PL rise components. The fast component (<<1 ns, barely noticeable in Fig. 1(b)) is determined by the direct carrier excitation in the DQW. The slow, ns-scale component reflects carrier transport from the cap layer to the DQW.

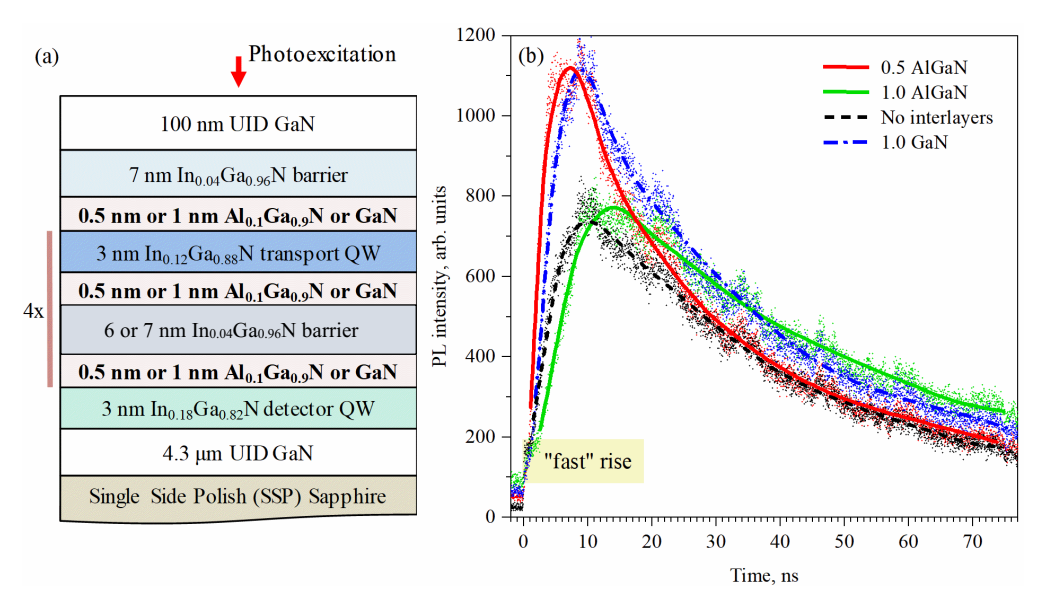


Figure 1. Schematics of the studied structures (a), DQW PL transients at 300 K (b).

The IW transport times were estimated by fitting of the PLtransients with the equation

$$I_{PL}(T) = A \left(\exp\left(-\frac{t - t_0}{\tau_r}\right) - \exp\left(-\frac{t - t_0}{\tau_d}\right) \right) + I_0,$$
(1)

where A is a proportionality coefficient, τ_r and τ_d are the slow PL rise and decay times, t_θ and I_θ are the time and intensity offsets, respectively. The τ_r , values, subsequently referred to as the IW transport times, are listed in Table I. Duration of the slow rise for all the samples is similar; hence, the interlayers do not cause a major hinder for the IW transport despite the large interlayer barrier height. Only for the structure with 1 nm AlGaN interlayers the IW transport time is prolonged

by a few ns with respect to the structure with no interlayers. Surprisingly, for the 0.5 nm AlGaN interlayer structure the IW transport is even faster than for the reference one.

Table 1. Tra	nsport and reco	mbination parame	eters for the st	udied structures a	at room temperature.
I dole I . I I d	insport und rece	minomation param	cters for the st	adica stractares t	at 100mm temperature.

Interlayers	0.5 nm AlGaN	1.0 nm AlGaN	1.0 nm GaN	No interlayers
IW transport time, ns	0.9	3.6	1.3	1.4
Radiative recombination time, ns	7.7	8.5	11.6	8.5
Nonradiative recombination time, ns	7.1	10.8	10.7	5.4
IQE, %	48	56	48	39

As mentioned, in InGaN multiple QW structures the IW transport is limited by the thermionic transport of holes, which consists of a sequence of capture into and thermionic emission out of the QWs.⁶ The effective energy for the hole thermionic emission E_{therm} consists of two components, the hole confinement energy and energy of the barrier tilt (see Fig.

3). Experimentally, the effective energy for the thermionic emission may be evaluated from the temperature dependence of the IW transport time. An Arrhenius-type plot of these times is shown in Fig. 2. An exponential decrease of the IW transport time with increasing temperature confirms that the thermionic hole emission is the limiting transport process also in the structures with interlayers. Activation energies, extracted from the slopes in Fig. 2, are similar for the four structures. This points out that the effective potential barrier for the thermionic hole transport is not affected by the interlayers. On the other hand, the IW transport times for the different structures are different (Table I) showing that the interlayers do influence the IW transport, even though not in a critical way. To get a deeper insight into these experimental observations, it is useful to analyze the band diagram.

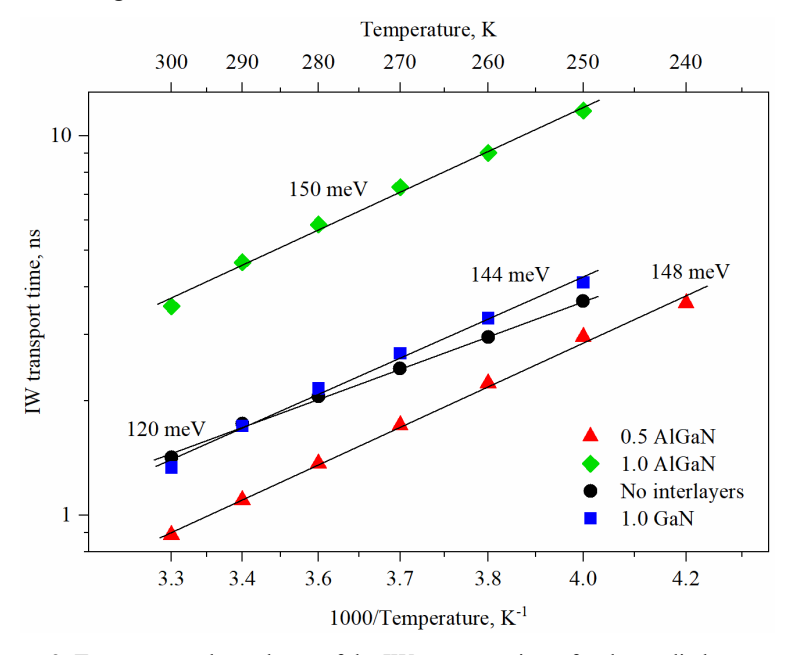


Figure 2. Temperature dependence of the IW transport times for the studied structures.

The valence band profile in the TQW region is shown in Fig. 3. It was calculated by self-consistently solving onedimensional Schrödinger and Poisson equations with a solver of Ref. 10. The solver does not consider local InGaN alloy composition and QW width fluctuations¹¹ as well as thickness variations of the interlayers. Nevertheless, it still provides information on the spatial band profiles and electron and hole wave functions.

The band diagrams show that, ignoring the interlayers, the activation energies for the hole thermionic emission for all structures are similar, just as observed experimentally. The measured and calculated values of these activation energies, however, are somewhat different, ~140 meV vs. ~220 meV. This difference suggests that holes overcome top of the barrier

by thermally-assisted tunneling. On the other hand, the discrepancy could be related to the different conditions for which the calculations and experiments were performed. The calculated band profile corresponds to a static situation with only electrons present in the TQWs. In the experiments, both electrons and holes are in the TQWs, their densities are rather high ($\sim 10^{18}$ cm⁻³) and these densities change with time. The photoexcited carriers in the QWs would partially screen the electric field and reduce the potential tilt in the barriers diminishing the effective energy for the thermionic transport. Additionally, natural alloy fluctuations in the InGaN and AlGaN layers may provide lower energy pathways for hole transport. ^{12,13} In any case, the calculated activation energies show no major dependence on the interlayer material and thickness confirming that the interlayers do not affect the thermionic transport. Therefore, transport through the interlayers with the thickness L_{IL} should be assigned to tunneling (in the barriers with the thickness L_B it remains diffusive). Since in different structures the interlayers have different thicknesses and barrier heights, one would expect the tunneling time τ_r to be different. In a semiclassical picture, the tunneling time through a potential barrier is defined as: ^{14,15}

$$\tau_{t} = \frac{2L_{B}}{\overline{v}_{B}} \exp \left[2L_{IL} \sqrt{\frac{2m_{IL}^{*} \Delta_{IL}}{\hbar^{2}}} \right]$$
 (2)

where \overline{v}_B is the average hole velocity in the barrier in the direction of the structure growth, m_{IL}^* is the hole effective mass in the interlayer, and Δ_{IL} is the interlayer barrier height. The calculated tunneling times for one interlayer are 1.5 ps, 3.6 ps and 14 ps for the 0.5 nm AlGaN, 1 nm GaN and 1 nm AlGaN interlayers, respectively. Considering just unidirectional carrier transport toward the DQW, the short tunneling time cannot account for the prolongation of IW transport time by ~2 ns for the structure with 1 nm AlGaN interlayers. However, during the IW transport the thermionic emission and tunneling take place both in the forward and backward direction, ¹⁶ increasing the number of emission and tunneling events required to reach the DQW, which would effectively prolong the IW transport time and possibly explain the experimental result. The puzzling effect of the shorter IW transport time for the 0.5 nm AlGaN structure compared to the no-interlayer structure could be assigned to the difference in the tunneling barriers for these structures. Assuming that the top of the barriers in the no-interlayer sample is also being overcome by tunneling, the thickness of this tunneling barrier could be considerably larger for the reference sample than for the one with 0.5 nm AlGaN interlayers (inset to Fig. 3). Since the barrier thickness has a larger impact on the tunneling time as the barrier height (see Eq. 2), the net effect might be the shorter tunneling time for the 0.5 nm AlGaN interlayer structure. In addition, the small interlayer thickness might not be uniform throughout the sample inducing paths for a faster interwell transport.

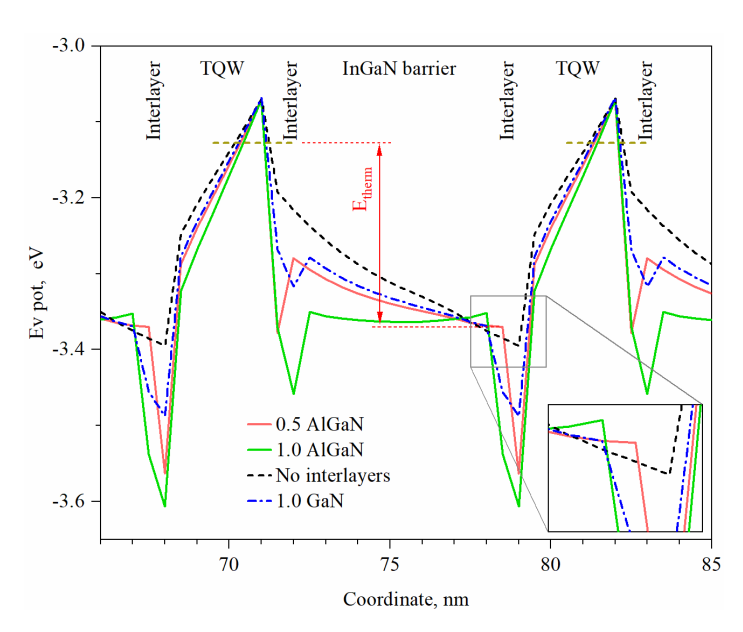


Figure 3. Valence band diagrams of studied samples at 300 K. The diagrams are aligned with respect to the ground state energy level of the left QW.

Now, let us examine the interlayer impact on recombination by evaluating the radiative and nonradiative recombination times and the IQE. The radiative recombination time at room temperature can be estimated from the ratio of PL transient amplitudes at room and low temperatures.^{17,18} If at low temperatures the inverse transient amplitude (proportional to the radiative recombination time τ_R) has the same temperature dependence as the PL decay time τ_{PL} , the IQE at low temperature is 100%, and the radiative recombination time can be determined in absolute values.¹⁷ In our case, such dependence was observed providing room temperature τ_R values listed in Table I. The nonradiative recombination time τ_{NR} (Table I) was calculated using the relation $1/\tau_{NR} = 1/\tau_{PL} - 1/\tau_R$, where τ_{PL} corresponds to the PL decay time shortly after the excitation. The IQE was then evaluated from $\eta = \tau_{NR} / (\tau_{NR} + \tau_R)$. Table I shows that in the samples with interlayers the nonradiative recombination times are longer, and the IQE is increased by about 10%. Reduction of the nonradiative recombination rate probably occurs due to decrease of the nonradiative recombination center density at the interfaces.¹⁹ In addition, the high band gap interlayers inserted at the well/barrier interfaces create potential barriers for the carrier capture from the wells to the nonradiative centers in the barriers and at the interfaces.²⁰

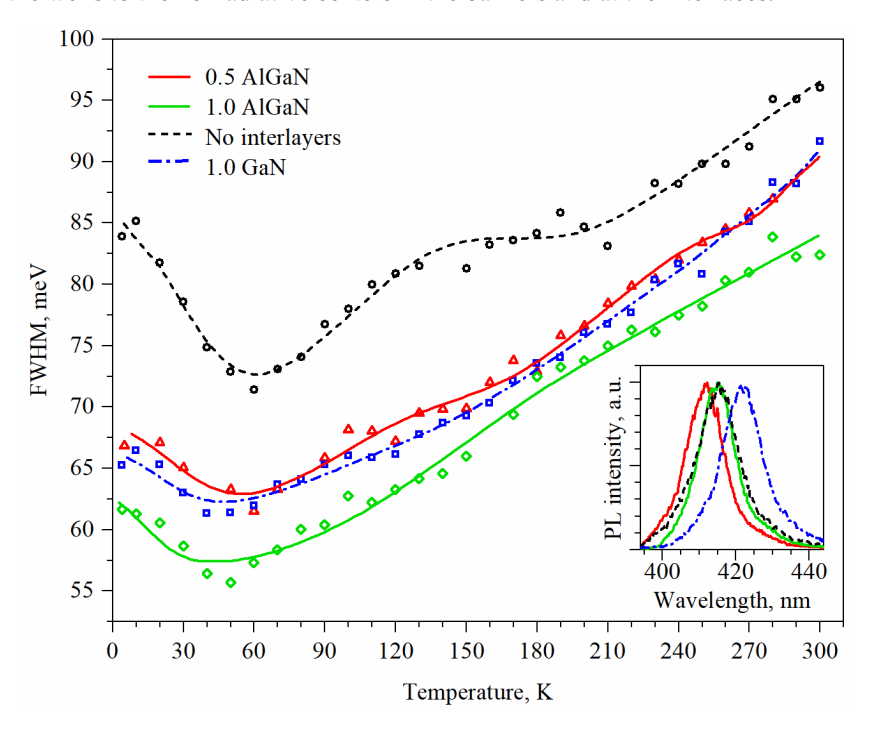


Figure 4. FWHM of PL spectra (inset) for transport QWs at different temperatures. The lines are a guide to the eye.

Another effect observed in the interfaced QW structures is narrowing of the QW PL peak (Fig. 4). In general, the shape of the temperature dependence of the full width at half maximum (FWHM) is determined by the carrier localization. ^{21,22} At low temperatures, carriers are localized in both shallow and deep potential fluctuations, and their distribution is nonthermal. With increasing temperature, carriers are thermally excited and transfer from the shallow to deep minima narrowing the spectrum. At even higher temperatures, carriers gain sufficient thermal energy to repopulate the shallow minima and higher energy states in the conduction and valence bands. What is important in the context of this work is that at all temperatures the FWHM for samples with interlayers is considerably narrower than that of the reference sample. In addition, the initial (4 K to 60 K) linewidth decrease for the interlayer structures is also smaller. This shows that the interlayers decrease the band potential fluctuations in the QWs. These fluctuations occur due to nm-scale variations of the InGaN alloy composition and QW width. ²³ In all our structures, the QWs were grown under identical conditions; thus, we assume that the alloy composition fluctuations are the same. The QW interfaces, however, are different. Consequently, our results suggest that the (Al)GaN interlayers at the In_{0.12}Ga_{0.88}N/In_{0.04}Ga_{0.96}N QW interfaces not only reduce the rate of the nonradiative recombination but also smoothen the interfaces reducing the linewidth of the emission peak. The latter feature might be especially useful for long wavelength InGaN QWs with a spectrally wide emission.

4. CONCLUSIONS

Efficient high-power operation of GaN-based multiple QW LEDs requires rapid interwell hole transport and low nonradiative recombination. In this work, we attempted to reduce the nonradiative recombination by introducing thin GaN or AlGaN interlayers at the In_{0.12}Ga_{0.88}N/In_{0.04}Ga_{0.96}N QW/barrier interfaces. It was found that the interlayers reduced the nonradiative recombination rate and increased the IQE by about 10%. Furthermore, the interlayers did not substantially slow down the interwell hole transport; for 0.5 nm Al_{0.10}Ga_{0.90}N interlayers the transport even became faster. The temperature dependent measurements show that during the interwell transport holes transfer through the interlayers via tunneling. Another positive feature of the interlayers is narrowing of the QW PL linewidth, which has been attributed to smoother QW interfaces.

ACKNOWLEDGMENTS

Research at KTH was financially supported by the Swedish Energy Agency (Contract No. 45390-1). Support at UCSB was provided by the Solid State Lighting and Energy Electronics Center (SSLEEC), the Simons Foundation (Grant No. 601952, J.S.S.), and the National Science Foundation (NSF) RAISE program (Grant No. DMS-1839077). Additional support for J.S.S. during preparation of this manuscript came from the U.S. DOE EERE (Grant No. DE-EE0009691).

REFERENCES

- [1] Kioupakis, E., Yan, Q., Steiauf, D., and Van de Walle, C. G., "Temperature and carrier-density dependence of Auger and radiative recombination in nitride optoelectronic devices," New J. Phys. 15, 125006 (2013).
- [2] Tran C. A., Osinski, A., Karlicek Jr., R. F., and Berishev, I., "Growth of InGaN/GaN multiple-quantum-well blue light-emitting diodes on silicon by metalorganic vapor phase epitaxy," Appl. Phys. Lett. 75, 1494 (1999).
- [3] Cao, X. A., LeBoeuf, S. F., Rowland, L. B., Yan, C. H., and Liu H., "Temperature-dependent emission intensity and energy shift in InGaN/GaN multiple-quantum-well light-emitting diodes," Appl. Phys. Lett. 82, 3614 (2003).
- [4] David, A., Grundmann, M. J., Kaeding, J. F., Gardner, N. F., Mihopoulos, T. G., and Krames, M. R., "Carrier distribution in (0001) InGaN/GaN multiple quantum well light-emitting diodes," Appl. Phys. Lett. 92, 053502 (2008).
- [5] Scheibenzuber, W. G.; and Schwarz, U. T., "Unequal pumping of quantum wells in GaN-based laser diodes", Appl. Phys. Express 5, 042103 (2012).
- [6] Marcinkevičius, S., Yapparov, R., Kuritzky, L. Y., Wu, Y.-R., Nakamura, S., DenBaars, S. P., and Speck, J. S., "Interwell carrier transport in InGaN/(In)GaN multiple quantum wells", Appl. Phys. Lett. 114, 151103 (2019).
- [7] Yapparov, R., Lynsky, C., Nakamura, S, Speck, J. S., and Marcinkevičius, S., "Optimization of barrier height in InGaN quantum wells for rapid interwell carrier transport and low non-radiative recombination," Appl. Phys. Express 13 122005 (2020).
- [8] Deveaud, B., Shah, J., Damen, T. C., Lambert, B., and Regreny, A., "Bloch transport of electrons and holes in superlattice minibands: Direct measurement by subpicosecond luminescence spectroscopy," Phys. Rev. Lett. 58, 2582 (1987).
- [9] Fröjdh, K., Marcinkevičius, S., Olin, U., Silfvenius, C., Stålnacke, B., and Landgren, G., "Interwell carrier transport in InGaAsP multiple quantum well laser structures," Appl. Phys. Lett. 69, 3659 (1996).
- [10] Hebal, H., Koziol, Z., Lisesivdin, S. B., and Steed R., "General-purpose open-source 1D self-consistent Schrödinger-Poisson Solver: Aestimo 1D," Comput. Mater. Sci. 186, 110015 (2021).
- [11] Yang, T.-J., Shivaraman, R., Speck, J. S., and Wu, Y.-R., "The influence of random indium alloy fluctuations in indium gallium nitride quantum wells on the device behavior," Appl. Phys. Lett. 116, 113104 (2014).
- [12] Browne, D. A., Mazumder, B., Wu, Y.-R., and Speck, J. S. "Electron transport in unipolar InGaN/GaN multiple quantum well structures grown by NH₃ molecular beam epitaxy," J. Appl. Phys. 117, 185703 (2015).
- [13] Qwah, K. S., Monavarian, M., Lheureux, G., Wang, J., Wu, Y.-R., and Speck, J. S., Theoretical and experimental investigations of vertical hole transport through unipolar AlGaN structures: Impacts of random alloy disorder," Appl. Phys. Lett. 117, 022107 (2020).
- [14] Köhler, K., Polland, H.-J., Schultheis, L., and Tu, C. W., "Photoluminescence of two-dimensional excitons in an electric field: Lifetime enhancement and field ionization in GaAs quantum wells," Phys. Rev. B 38, 5496 (1988).
- [15] Le Tomas, N., Pelekanos, N. T., and Hatzopoulos, Z., "Selective measurement of hole tunneling times through AlGaAs barriers based on the quantum confined Stark effect," Phys. Rev. B 72, 235323 (2005).

- [16] Toprasertpong, K., Goodnick, S. M., Nakano, Y., and Sugiyama, M., "Effective mobility for sequential carrier transport in multiple quantum well structures," Phys. Rev. B 96, 075441 (2017).
- [17] Hangleiter, A., Langer, T., Henning, P., Ketzer, F. A., Bremers, H., and Rossow U., "Internal quantum efficiency of nitride light emitters: A critical perspective," Proc. SPIE 10532, 105321P (2018).
- [18] Marcinkevičius, S., Yapparov, R., Chow, Y. C., Lynsky, C., Nakamura, S., DenBaars, S. P., and Speck, J. S., "High internal quantum efficiency of long wavelength InGaN quantum wells," Appl. Phys. Lett. 119, 071102 (2021).
- [19] Hetzl, M., Winner, J., Francaviglia, L., Kraut, M., Döblinger, M., Matich, S., Fontcuberta i Morral, A., and Stutzmann, M., "Surface passivation and self-regulated shell growth in selective area-grown GaN–(Al,Ga)N core–shell nanowires," Nanoscale 9, 7179 (2017).
- [20] Peng, M., Zheng, X., Liu, S., Wei, H., He, Y., Li, M., An, Y., Song, Y., and Qiu, P., "A large-scale, ultrahigh-resolution nanoemitter ordered array with PL brightness enhanced by PEALD-grown AlN coating," Nanoscale, 11, 3710 (2019).
- [21] Pecharromán-Gallego, R., Martin, R W., and Watson, I. M., "Investigation of the unusual temperature dependence of InGaN/GaN quantum well photoluminescence over a range of emission energies," J. Phys. D: Appl. Phys. 37, 2954 (2004).
- [22] Marcinkevičius, S., Gelžinytė, K., Zhao, Y., Nakamura, S., DenBaars S. P., and Speck, J. S., "Carrier redistribution between different potential sites in semipolar (20-21) InGaN quantum wells studied by near-field photoluminescence," Appl. Phys. Lett. 105, 111108 (2014).
- [23] Dawson, P., Schulz, S., Oliver, R. A., Kappers, M. J., and Humphreys, C. J., "The nature of carrier localisation in polar and nonpolar InGaN/GaN quantum wells," J. Appl. Phys. 119, 181505 (2016).